Analytical Axisymmetric Coupled Piezo-Elastodynamic Models for Guided-Wave Structural Health Monitoring

Christopher T. Dunn, Ajay Raghavan and Seth S. Kessler
Metis Design Corporation

IWSHM-2009

ABSTRACT

With guided-wave approaches becoming prevalent for structural health monitoring, the need has arisen for more effective models employing these methods using piezoelectric transducers. This paper describes an analytical formulation to couple transducer dynamics with axisymmetric guided-wave excitation models for isotropic plates. The finite-dimensional piezo-actuator dynamics are modeled using coupled piezoelectricity-elasticity equations, assuming the actuators thickness is small compared to its in-plane dimensions. The surface-bonded actuator is assumed to cause a shear traction on the structural substrate along the actuator's edge. The amplitude of the exerted shear traction is computed by matching the traction and displacement at the actuator's edge with that of the structure, taking into consideration the structural contributions from all possible guided-wave modes. The structural guided-wave response is computed using axisymmetric elasticity based model developed earlier with the piezo-actuator's computed shear traction as the excitation function. The theoretical predictions from this approach are compared with results from corresponding finite element simulations for various frequencies and actuator thicknesses.

INTRODUCTION

Guided-wave (GW), also known as Lamb-wave, approaches have emerged as a promising solution for structural health monitoring (SHM) in recent years. Structures are excited with high frequency GWs, the difference in their response with respect to a baseline signal are processed, and algorithms can be trained to detect and characterize damage. The main advantages of GW methods over other

Christopher T. Dunn, Metis Design Corporation, 10 Canal Park, Cambridge, MA 02141
Ajay Raghavan, Metis Design Corporation, 10 Canal Park, Cambridge, MA 02141
Seth S. Kessler, Metis Design Corporation, 10 Canal Park, Cambridge, MA 02141

methods are their ability to interrogate large structural areas and locate/characterize damage on demand with a sparse network of transducers. Most commonly, piezoelectric transducers (piezos) are used for GW excitation and sensing. A detailed description of GW SHM, its basic principles and a summary of efforts by other researchers have been presented in Raghavan and Cesnik [1]. Reliable models for GW excitation/sensing are important for efficient design of GW SHM systems and algorithms. This is because the interpretation of GW signals can be complicated by their dispersive, multimodal nature. Earlier efforts in this direction for piezoelectric actuators have largely examined reduced structural theories or 2-D plane strain models [2]. Raghavan and Cesnik developed 3-D elasticity models for GW excitation and sensing, however their work assumes uncoupled piezo-structural dynamics [3,4]. This implicitly assumes that the shear traction exerted by the piezo on the structure is independent of frequency. It also implies that at least one calibration experiment/coupled finite element simulation is needed for each piezo-structural material combination to estimate this traction. Only some limited mathematical work in the literature has examined coupled piezo-elastodynamic models for GW excitation, which assume plane strain [5]. Thus, the developed models in the open literature are restricted in their applicability for transducer design, either leaving out transducer dynamics or the third dimension.

The present paper seeks to bridge this gap by proposing an analytical formulation to couple the finite-dimensional piezoelectric transducer dynamics with earlier axisymmetric GW excitation models for isotropic plates. The piezo-actuator dynamics are modeled using coupled piezoelectricity-elasticity equations, assuming its thickness is small compared to its in-plane dimensions. This is a reasonable assumption for most practical structural health monitoring applications. The piezo-actuator is assumed to cause a shear traction on the structural substrate surface along the actuator's edge. The amplitude of the exerted shear traction is computed by matching the traction and displacement at the piezo's edge with that of the structure, taking into consideration the structural contributions from all possible GW modes. The structural GW response is computed using axisymmetric models developed earlier with the piezo-actuator's computed shear traction as the excitation function [5]. The results of this approach are compared with those from corresponding finite element simulations. Finally, the validity of some of the model's assumptions is examined and the use of these models for designing more effective structural health monitoring systems is discussed.

PROBLEM FORMULATION

Consider a piezoelectric disk actuator bonded to an infinite plate structure, as shown in Figure 1. The r, θ, z coordinate system is a cylindrical coordinate system with the r axis pointing in the plane of the structure, and the z axis along the out-of-plane direction. The structure is of thickness $2b$, and actuator is of thickness h_{Act} and radius a respectively. The actuator is poled in the z direction and is electroded on the z surfaces. The actuator is driven using a voltage $V_{Act}(t)$, and a current $i_{Act}(t)$ is induced. As can be seen, the actuator voltage and current follow the passive sign convention. The actuator and structure is joined at $r = a$, as will be described in a later section of this paper.

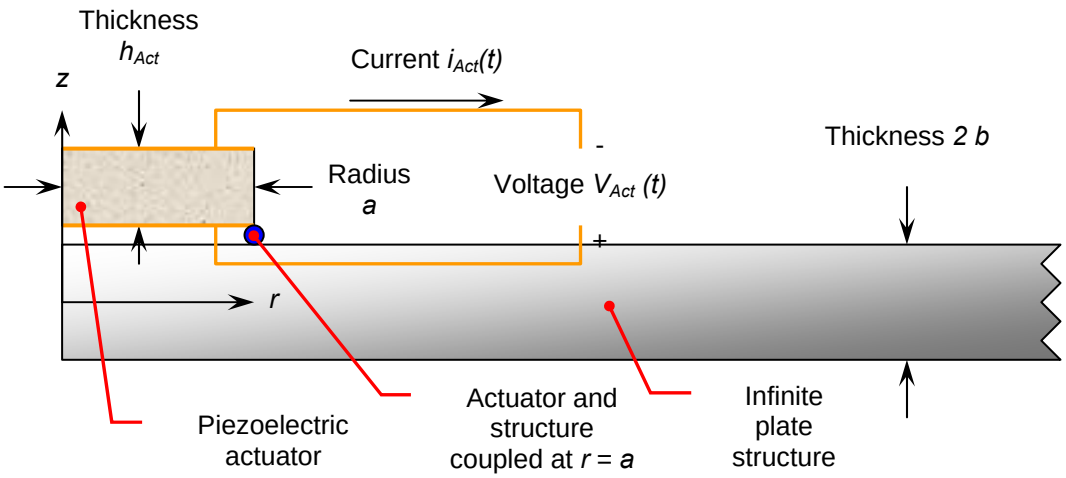

Figure 1. Axisymmetric view of a piezoelectric actuator bonded to an infinite structure

MODELS

The following is a discussion of the closed-form structural and actuator models and the approximations used to couple the two together. The finite element model of the actuator/structure system is also discussed.

Structure

The structural response of an isotropic plate of thickness 2*b* with a surface bonded circular actuator of radius *a* exerting shear traction of magnitude τ_{Str}, can be found in Raghavan and Cesnik [5]. The problem is solved by applying the Hankel transform along the radial axis *r* to the 3-D elasticity equations and using residue calculus to recover the spatial domain solution. The harmonic surface radial displacement at radius *r* can be shown to be:

$$u_r(r,b) = j\pi \frac{\tau_{Str}\, a}{\mu} e^{j\omega t} \left[\begin{array}{l} \sum_{\xi^S} J_1(\xi^S a) N_S(\xi^S) H_1^{(2)}(\xi^S r) / D_S'(\xi^S) \\ + \sum_{\xi^A} J_1(\xi^A a) N_A(\xi^A) H_1^{(2)}(\xi^A r) / D_A'(\xi^A) \end{array} \right] \quad (1)$$

where λ and μ are the Lamé's constants of the plate, which has material density ρ, $J_n(\,)$ is the Bessel function of order *n*, $H_n^{(2)}(\,)$ is the Hankel function of the second type and order *n*, ξ is the wavenumber, *j* is the square root of negative one, the prime represents the derivative, and the super/sub-scripts *A* and *S* respectively correspond to the antisymmetric and symmetric Lamb modes. The summation is performed over all possible Lamb and evanescent modes, (although the evanescent modes tend to have negligibly small contributions). It should be noted that the other possible GWs for the isotropic plate, namely, the horizontal shear (SH) modes, are not excited in this case. The other terms in Equation 1 are:

$$
\begin{aligned}
N_S &= \xi\beta\left(\xi^2+\beta^2\right)\cos(\alpha b)\cos(\beta b)\\
D_S &= \left(\xi^2-\beta^2\right)^2\cos(\alpha b)\sin(\beta b)+4\xi^2\alpha\beta\sin(\alpha b)\cos(\beta b)\\
N_A &= \xi\beta\left(\xi^2+\beta^2\right)\sin(\alpha b)\sin(\beta b)\\
D_A &= \left(\xi^2-\beta^2\right)^2\sin(\alpha b)\cos(\beta b)+4\xi^2\alpha\beta\cos(\alpha b)\sin(\beta b)\\
\alpha^2 &= \omega^2/c_1^2-\xi^2 \qquad c_1=\sqrt{(\lambda+2\mu)/\rho}\\
\beta^2 &= \omega^2/c_2^2-\xi^2 \qquad c_2=\sqrt{\mu/\rho}
\end{aligned}
\tag{2}
$$

The wavenumber ξ specific mode for angular frequency ω is obtained from the solutions of the Rayleigh-Lamb equation for free waves in an isotropic plate:

$$
\tan(\beta b)/\tan(\alpha b)=\left[-4\alpha\beta\xi^2/\left(\xi^2-\beta^2\right)^2\right]^{\pm 1} \tag{3}
$$

where the positive and negative exponents are for the symmetric and antisymmetric Lamb modes respectively.

Piezoelectric actuator

Consider a disk of radius a and thickness h_{Act} comprised of a class 6 mm piezoelectric material, such as PZT-5A [6]. Let us assume the disk is driven on the edge using a radial force, $F_{Act}(t)$, with a resulting velocity $\dot{u}_{Act}(t)$ and excited with a voltage $V_{Act}(t)$ with a resulting current $i_{Act}(t)$. If it is assumed that the material is stress free through the thickness, there is no fringing of the electric field, and displacements are axisymmetric and independent of the z-coordinate, then the solution is that of a radial mode for a thin piezoelectric disk [7]. The relationship between the edge force, edge velocity, voltage, and current for the piezoelectric actuator in the spectral domain is given by:

$$
\begin{Bmatrix} F_{Act}(\omega) \\ V_{Act}(\omega) \end{Bmatrix} = \begin{bmatrix} Z_{11}^{Act}(\omega) & Z_{12}^{Act}(\omega) \\ Z_{12}^{Act}(\omega) & Z_{22}^{Act}(\omega) \end{bmatrix} \begin{Bmatrix} \dot{u}_{Act}(\omega) \\ i_{Act}(\omega) \end{Bmatrix} \tag{4}
$$

Where the impedances, Z_{ij}^{Act}, are given by:

$$
\begin{aligned}
Z_{11}^{Act} &= 2\pi j h_{Act}\left(\left[\left(c_{11}^P-c_{12}^P\right)\varepsilon_{33}^P-2\left(e_{31}^P\right)^2\right]/\left[\varepsilon_{33}^P\omega\right]-a c_{11}^P J_0\left(a\omega/v^P\right)/\left[v^P J_1\left(a\omega/v^P\right)\right]\right)\\
Z_{12}^{Act} &= 2j e_{31}^P h_{Act}/\left(a\varepsilon_{33}^P\omega\right) \quad Z_{22}^{Act} = h_{Act}/\left(j\omega\varepsilon_{33}^P\pi a^2\right)
\end{aligned}
\tag{5}
$$

where c^P, e^P, v^P, and ε^P are the planar piezoelectric material properties [8].

Approximation joining the structural model to the actuator model

To couple the structural model to the actuator model, let us assume the two are only joined at $r = a$. Consider the free body diagram of the piezoelectric disk actuator and infinite plate structure, as shown in Figure 2.

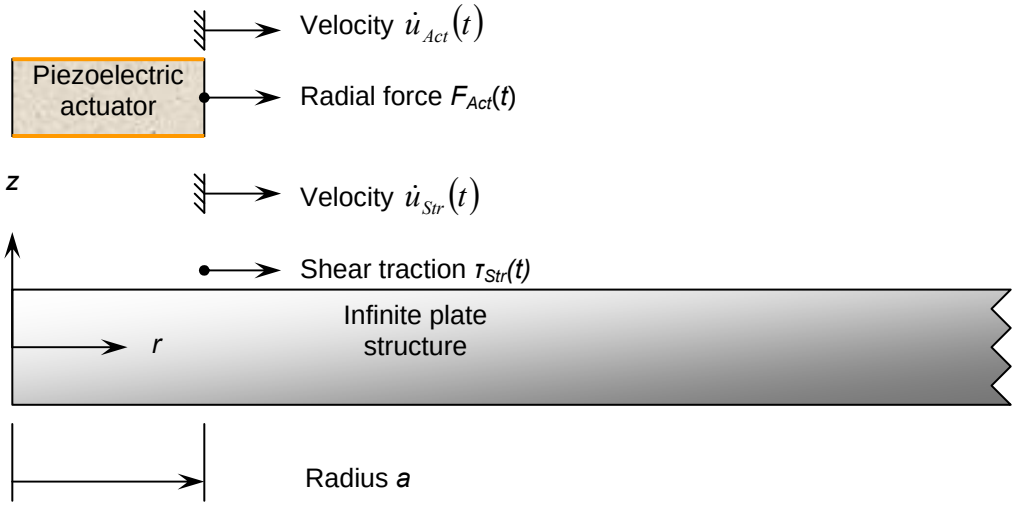

Figure 2. Free body diagram of the actuator / structure system

On the edge of the actuator, at $r = a$, is applied an outward radial force F_{Act}. This force causes a velocity at the edge of the actuator of $\dot{u}_{Act}$. On the top surface of the structure at $r = a$ is a shear traction τ_{Str}, which results in a reaction velocity of $\dot{u}_{Str}$. Summing forces at $r = a$:

$$F_{Act}(t) = -2\pi a \tau_{Str}(t) \tag{6}$$

Due to continuity of the displacement at $r = a$:

$$\dot{u}_{Act}(t) = \dot{u}_{Str}(t) \tag{7}$$

The implications of the approximation that the actuator and structure are coupled only at one point will be discussed in the discussion section.

Finite element model

A 2-D axisymmetric finite element model of the actuator and structure was constructed in Ansys 11 [8]. The actuator was meshed with 8-node "plane 223" piezoelectric elements with voltage and displacement degrees of freedom. The structure was meshed with 8-node structure elements with displacement degrees of freedom. The model consisted of between 8,440 and 37,056 elements and 29,537 and 129,669 nodes with four elements through the thickness. The response of the plate was simulated in time domain using a transient analysis. The actuator electrodes were simulated by coupling the voltage degrees of freedom along the respective electrode surface. The actuator was driven using a 3.5 cycle, 1 V amplitude sinusoidal wave modulated by a Hanning window. The simulations were done over a range of center frequencies from 10 to 200 kHz in 10 kHz increments and from 220 kHz to 500 kHz in 20 kHz increments. At each time step, actuator voltage, actuator charge, and structural displacements were recorded. To avoid boundary reflections (which are not captured in the infinite structural model), the outer diameter of the structure was chosen such that the fastest wave (S_0 wave) would just hit the outer diameter of the structure at the end of the analysis.

RESULTS

The closed form was derived in the spectral domain and the finite element model was solved in the time domain. To convert from the spectral to the time domain, the discrete inverse Fourier transform was used. The results from the closed form model and finite element simulations are compared in the following plots. Unless noted, the following plots are for a 2.54 cm (1") diameter × 254 μm (10-mil) thick PZT-5A actuator bonded to a 3.2 mm (0.125") thick aluminum 6061-T6 structure. The results for the actuator current for the closed form and finite element models are compared in Figure 3. It can be seen in this figure that the closed form solution and the finite element model match very well both in the time and frequency domain. The largest disagreement in the slope in the frequency domain (~6%) occurs for the thinnest actuator (5 mils).

The plots of peak-to-peak displacement for two actuator thicknesses at a radial position of 30 cm (12") versus the actuator center frequency are shown in Figure 4. In this figure it can be seen that the closed-form solution is in agreement with the finite element solution, except near piezo resonance and above 200 kHz for the S_0 mode of the 30 mil thick actuator. For the A_0 mode, the closed form and finite element models agree well over the range of frequencies. The contributions of the S_0 and A_0 mode in the finite element results for radial displacement were calculated by taking the sum and difference of the values on either free surface at the same r location.

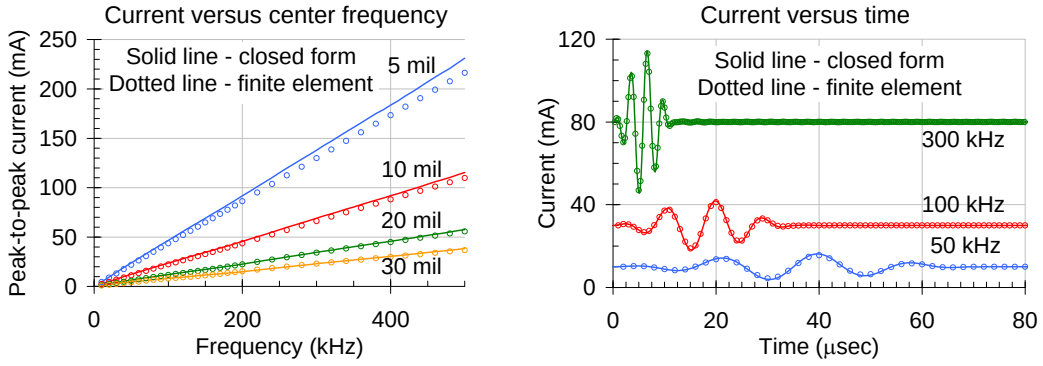

Figure 3. Current versus center frequency and time (DC offset added for clarity)

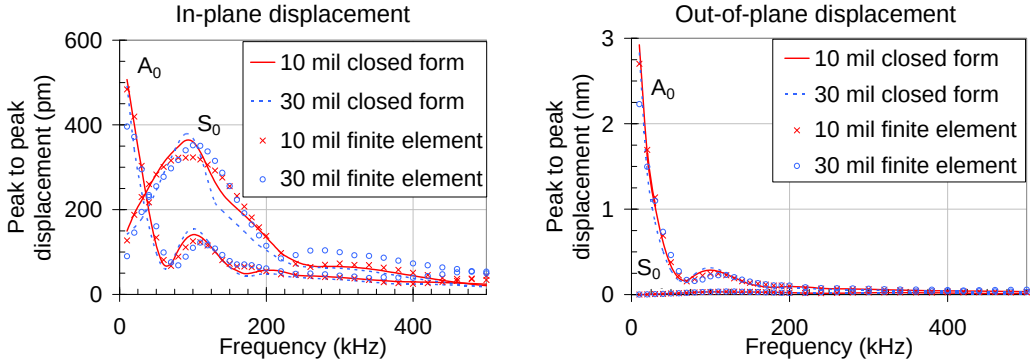

Figure 4. Surface displacement at r = 30 cm (12") versus center frequency

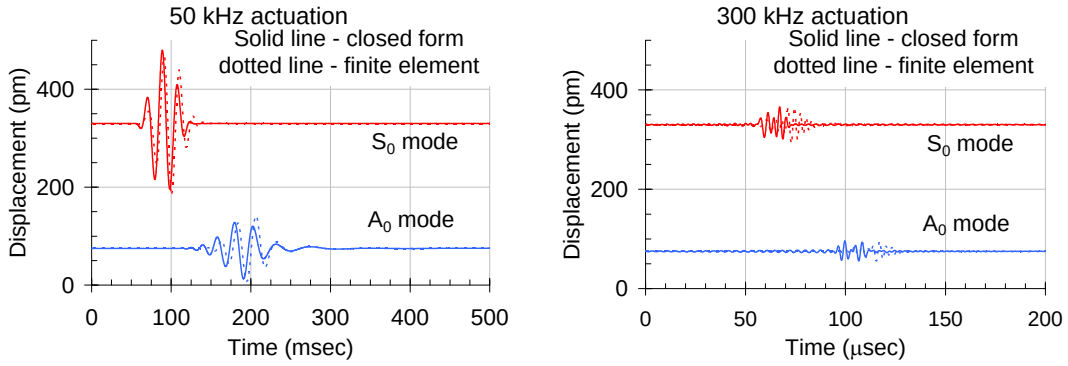

Figure 5. In-plane surface displacement at r = 30 cm (12") versus time (DC offset added for clarity)

The in-plane displacements at a radial position of 30 cm (12") versus time are compared in Figure 5. At 50 kHz the finite element and closed form solution agree well. At higher center frequencies however, the two solutions are less in agreement, with the closed-form solution leading the finite element solution by about 20 μs. However, the relative amplitudes are still captured well by the model.

DISCUSSION ON COUPLING ASSUMPTION

To understand some minor discrepancies at higher frequencies (> 300 kHz), it is useful to examine the validity of a key assumption made in coupling the piezoelectric actuator model with the structural model, namely, regarding the shear traction exerted on the structure. The *zz* and *rz* stress at the actuator / structure interfaces versus the radial position from the finite element simulation are plotted in Figure 6. It should be noted that in Figure 6, the stresses are plotted at the instant when the actuator is being driven using the peak voltage. For low frequencies, both stresses are approximately zero over most of the actuator except at the edge, where the normal stress is negligible compared to the shear stress. This is the consistent with the assumptions of the closed form model, and the reason for its good a agreement with the finite element model at lower frequencies. For higher frequencies, while the shear stress at the edge is still dominant, the stresses are small but not negligible over the actuator length, and the agreement between the closed form and finite element model is weaker for the time domain results.

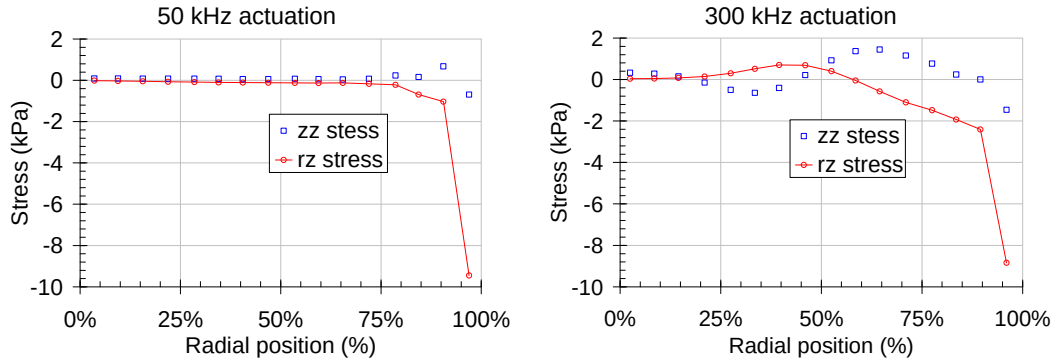

Figure 6. Stress at the actuator/structure interface versus position (% of actuator radius) from FEM

CONCLUDING REMARKS

In summary, this paper presented a theoretical model to predict the guided-wave response of isotropic plates driven by surface-bonded piezoelectric wafer actuators. The model captures both the piezoelectric actuator dynamics and all possible guided-wave modes in the structure. The model's predictions were compared to results from corresponding finite element simulations with good agreement. The model can be used as an effective tool for SHM system design. One could examine the effect of parameters such as actuator and structural dimensions and materials on the SHM system range, electrical power drawn by the actuator, prediction of the actuator resonance, etc. Crucially these are achieved without the need for experimental/finite element calibration, unlike earlier models. It also offers significant advantages in computation time over finite element analysis.

Future modeling directions for this work include examining higher fidelity models for the piezo, which could incorporate the out-of-plane stresses for higher frequencies, as well as extending the model for ring-shaped/rectangular piezos and composite structures. Other areas of future planned research include the incorporation of material damping/attenuative factors and coupled sensor responses into these models, in order to produce a closed-form tool to facilitate sensor layout and density optimization.

REFERENCES

1 Raghavan A. and Cesnik C.E.S., 2007. "Review of guided-wave structural health monitoring," *Shock and Vibration Digest*, 39(2): pp. 91-114.

2 Lin X. and Yuan F. G., 2001. "Diagnostic Lamb waves in an integrated piezoelectric sensor/actuator plate: analytical and experimental studies," Smart Materials and Structures v. 10, pp. 907–913, 2001.

3 Raghavan, A. and Cesnik, C.E.S., 2004."Modeling of piezoelectric-based Lamb-wave generation and sensing for structural health monitoring," *Proceedings of the SPIE*: 5391-42.

4 Raghavan, A. and Cesnik, C.E.S., 2005. "Finite dimensional piezoelectric transducer modeling for guided wave based structural health monitoring," *Smart Materials and Structures*, 14:1448-1461.

5 Glushkov, E.V., Glushkova, N.V., Seemann, W. and Kvasha, O.V., 2006. "Elastic wave excitation in a layer by piezoceramic patch actuators," *Acoustical Physics*: 52(4).

6 Berlinecourt D., Krueger, H.H.A., and Near, C. "Properties of Piezoelectricity Ceramics", Morgan Electro Ceramics, Technical Publication TP-226.

7 "IEEE Standard on Piezoelectricity", Institute of Electrical and Electronics Engineers, Inc, ANSI/IEEE Std 176-1987, pp. 39 – 41.

8 ANSYS 11 User's Manual, ANSYS, Inc, Canonsburg PA.